SQUEEZED PULSED LIGHT FROM A FIBER RING INTERFEROMETER

K. Bergman and H. A. Haus

Department of Electrical Engineering and Computer Science
and Research Laboratory of Electronics,
Massachusetts Institute of Technology, Cambridge, MA 02139

ABSTRACT

Observation of squeezed noise, 5±0.3 dB below the shot noise level, generated with pulses in a fiber ring interferometer is reported. The interferometric geometry is used to separate the pump pulse from the squeezed vacuum radiation. A portion of the pump is reused as the local oscillator in a homodyne detection. The pump fluctuations are successfully subtracted and shot noise limited performance is achieved at low frequencies (35-85 KHz). A possible utilization of the generated squeezed vacuum in improving a fiber gyro's signal to noise ratio is discussed.

INTRODUCTION

Squeezing in a fiber was first demonstrated by Shelby et al. [1] who showed that the fiber's $\chi^{(3)}$ nonlinearity could be used to shape the field's fluctuations through self phase modulation. The group's experimental results were, however, severely limited by acoustic and thermal noise processes. First, the low Stimulated Brillouin Scattering (SBS) threshold in fibers forced the IBM group to separate their CW pump into 25 frequency components. The second noise source, more difficult to avoid, was the so called GAWBS (Guided Acoustic Wave Brillouin Scattering) excitations [2]. GAWBS is caused by thermal fluctuations that modulate the fiber's refractive index at high frequencies (approximately between 20 MHz and 10 GHz) and thereby scatter acoustic waves which are guided in the forward direction. Because the experiment was performed in a traveling wave geometry, it was necessary to detect the squeezing at high frequencies (50-100 MHz) where the laser noise is negligible. The measurement center frequency was within the frequency range of GAWBS, and only about 12% of noise reduction was thus observed.

To improve upon these earlier results, we used short pulses in a fiber interferometer configuration. Large nonlinear phase shifts of the order of several π are easily achieved with short pulses of high peak power, while the SBS threshold is avoided. The fiber ring geometry is used to separate the pump from the squeezed vacuum fluctuations. Subsequent detection with a balanced detector permitted complete cancellation of the pump fluctuations at frequencies as low as 35-85 KHz. Although the GAWBS noise can be frequency down-converted into the detection "window" when pulses are used [3], it did not seem to prevent the noise reduction in our experiment. The investigation of the down-conversion of GAWBS requires further study.

The experimental results reported in this paper have been recently published [4]. This paper begins with a brief review of the broadband squeezing process in a fiber. Following the approach of Shirasaki and Haus [5], we then show how the pump is separated from the squeezed vacuum when the squeezing is performed within a Mach-Zehnder interferometer. The squeezed vacuum is observed with the aid of a local oscillator derived from the pump. We describe some of the theoretical limitations on the observed squeezing using homodyne detection and a gaussian shaped local oscillator. The experiment and results are then described in detail.

SQUEEZING IN THE NONLINEAR MACH-ZEHNDER

We consider the simple propagation equation for the field operator, $\hat{a}(z)$, in a nonlinear Kerr medium. Assuming no dispersion this equation becomes:

$$\frac{d\hat{a}(z)}{dz} = i\kappa[\hat{a}^{+}(z)\hat{a}(z)]\hat{a}(z) \tag{1}$$

where κ is the Kerr nonlinearity. The Kerr nonlinearity is calculated as follows,

$$\kappa = \frac{2\pi}{\lambda} n_2 \frac{P_p}{A_{eff}} \tag{2}$$

where λ is the wavelength, n_2 the nonlinear index, P_p the peak power, and A_{eff} the effective coupling area. Equation (1) may be integrated directly, yielding a solution for the field operator, $\hat{a}(z)$, after a propagation distance, L:

$$\hat{a}(L) = e^{i\kappa L\hat{a}^{+}(0)\hat{a}(0)}\hat{a}(0) \tag{3}$$

The effect of the Kerr medium is to add a nonlinear phase shift proportional to the photon number, propagation distance, and Kerr coefficient. The mean square fluctuations of the field are shaped by this nonlinear process as shown in figure 1. The $\chi^{(3)}$ process couples the amplitude and the phase fluctuations, causing the phase insensitive mean square fluctuations of the incoming field, represented by a circle, to stretch into an ellipse along the amplitude tangents. The area of the resulting squeezed noise ellipse is equal to the area of the initial circle.

Next, we place two equal lengths of Kerr media symmetrically in the two arms of a Mach-Zehnder interferometer, as was analyzed in reference [5]. The input field and its associated fluctuations enter one input port of the interferometer's first beam splitter in figure 2. Into the second, unexcited port enter the zero point fluctuations of the vacuum field. The field's amplitude split coherently in two by the 50/50 beam splitter. The fluctuations add and subtract incoherently.

As each field-half propagates through its Mach-Zehnder arm, it accumulates a nonlinear phase shift (not shown on the phasors in figure 2) and its fluctuation circles are stretched into ellipses. At the second beam splitter, the two half-field amplitudes interfere coherently. Under a linearized first order analysis, the squeezed fluctuations will again add and subtract incoherently. As illustrated with the phasors in figure 2, the original mean

field amplitude emerges from the constructive interference port, and the squeezed vacuum exits from the destructive interference port. The interferometer has made possible this isolation of the squeezed vacuum.

The above explanation for a single frequency phasor (CW pump) also holds for the case of a pulsed pump, as long as dispersion may be neglected. Without dispersion the pulse may be divided into short time segments and each segment analyzed independently. At the output the segments are superimposed to reconstruct the pulse.

DETECTION

The function of homodyne detection is to measure one quadrature of the incoming signal, amplified by the local oscillator. This detection technique is used to observe the phase sensitive fluctuations of the squeezed vacuum signal. If the local oscillator phase is properly adjusted, the squeezed (reduced noise) quadrature is measured. The fluctuations accompanying the pump are completely subtracted by the balanced detection. When the signal arm is blocked, the homodyne detection measures the vacuum state noise. This is a part of the experimental shot noise calibration.

In the Mach-Zehnder squeezing geometry, the exiting pump, shown in figure 2, may be reused as the local oscillator. In this way, the local oscillator pulse shape matches the squeezed vacuum pulse. However, to detect the full pulsed squeezing magnitude a finer matching of the local oscillator phase is required since the squeezing direction as well as magnitude will vary along the pulse duration. Thus, under ideal conditions the local oscillator should be phase shifted in one direction at the pulse center but in a different direction at the pulse wings. Experimentally the local oscillator is shifted by one constant phase leading to a nonideal measured noise reduction magnitude. We have plotted the expected noise reduction for the ideal and single phase adjusted gaussian pulse cases in figure 3 (a). In figure 3(b) we show that for the gaussian pulse case, the amplified noise amplitude is larger than the attenuated noise amplitude for the same peak nonlinear phase level.

EXPERIMENT

The experiment was implemented by replacing the Mach-Zehnder with a fiber ring interferometer, to take advantage of the ring's stability to vibrational and thermal disturbances. Figure 4 is a schematic of the experimental arrangement. A mode-locked 1.3μm Nd:YAG producing 100 psec pulses at a repetition rate of 100 MHz was used as the pump. This pulse train pump is coupled into the fiber ring reflector composed of 50 m of PM (polarization maintaining) fiber which is spliced to the two pigtails of a 3 dB PM fiber coupler. The coupler's splitting ratio was variable, and was carefully adjusted to 50/50 within 1 part in 500. The pump pulses are thus completely reflected from the ring. A 90/10 beam splitter picks off a portion of the reflected pump to be reused as the local oscillator. The squeezed vacuum signal emerges from the unexcited transmission port of the ring.

The local oscillator and the squeezed signal are then mixed in a 50/50 beam splitter (BS2), and detected with a balanced dual detector receiver. The output difference current is directly fed into a spectrum analyzer. The Power Spectral Density (PSD) reading

corresponds to a measure of the fluctuations magnitude along one quadrature of the squeezed vacuum. The amplified and reduced noise quadratures may now be measured by adjusting the relative phase of the local oscillator and squeezed signal.

The reduced noise will increase with the pulse peak nonlinear phase shift, which can be estimated from the following CW equation,

$$\Phi_{NL} = \frac{2\pi}{\lambda} n_2 L \frac{P_p}{A_{eff}} \tag{4}$$

where n_2 is the nonlinear index, L the fiber length, P_p the pulse peak power, and A_{eff} the effective coupling area. In this experiment, a peak nonlinear phase shift of 1.4 radians corresponds to approximately 100 mW of average power in each ring direction. The PSD measurements were performed at a narrow low frequency window between 39 and 41 KHz. Data was taken with an integration time of 400 msec and a frequency resolution of 2.5 Hz. Before discussing the results, we describe the methods used to calibrate the shot noise level.

IV SHOT NOISE CALIBRATION

The shot noise level was calibrated in order to confirm that the reduced quadrature fluctuations of the squeezed vacuum dropped below the zero point fluctuations level. Two methods were used. First, direct excitation from the laser was sent through the homodyne detection system and the detector current along with a corresponding PSD level were recorded for a range of input power levels. To cross check this calibration, two white light sources were used to generate detector current levels similar to those obtained with the laser excitation. Again, the PSD levels were recorded along with the current readings for the same range of power levels. The spectrum analyzer's noise floor was measured at -155 dBm/Hz and typical shot noise levels ranged from -120 to -125 dBm/Hz, so that electrical noise was not a factor. The two curves plotted on a dB scale in figure 5 overlapped well with a 45 degree slope. Thus, the laser noise has been successfully subtracted and the detection's response has been shown linear within the measurement current range.

V EXPERIMENTAL RESULTS

Having accurately established a shot noise level, we proceed with the squeezing measurement. The local oscillator pulse and the squeezed vacuum pulse are aligned to overlap spatially and temporally at the detection beam splitter (BS2). For alignment purposes only, the signal magnitude may be temporarily increased by changing the coupler's splitting ratio. The coupler is adjusted back to 50/50 and the relative phase between the local oscillator and squeezed signal is allowed to drift. While the phase is drifting, PSD measurements are taken continuously with an automated data acquisition system.

The PSD level, a measurement of the squeezed noise will vary from some maximum value to some minimum value corresponding to the amplified and attenuated quadratures of the squeezed vacuum. The resulting histograms from these measurements taken at three separate pump power levels: 60, 85, and 110 mW (in each fiber ring direction) are shown in figure 6 (a), (b), and (c) respectively. In the figure, the black bars are PSD readings taken with the squeezed vacuum arm blocked, and are thus the shot noise calibration for the specific power level. The white bars are a collection of PSD readings taken after the mixing of the local oscillator and squeezed vacuum. The reduced noise level or squeezing magnitude is defined as the distance between the black bars distribution center and the left edge of the white bars distribution. We note that as previously predicted for the case of a gaussian local oscillator, the amplified quadrature noise is larger than the reduced quadrature for the same power level.

In figure 7 we plot the experimental maximum and minimum PSD readings (in dot scatter format) obtained for a collection of power levels, on top of the theoretically predicted limits for the gaussian local oscillator case. The experimental point plot was adjusted horizontally, along the peak nonlinear phase axis for a best fit. This fitting compensates for coupling losses, detector quantum efficiencies, and nonlinear phase estimation.

VI SQUEEZED VACUUM IN A FIBER GYRO

It has been shown both theoretically [6,7,8], and experimentally [9,10], that the sensitivity of a phase measurement device can be improved with the injection of squeezed vacuum into the unexcited port. Normally, zero point fluctuations enter this unexcited port. We briefly consider the circumstances of utilizing the squeezed vacuum generated by the interferometric fiber ring to improve the performance of a second fiber ring functioning as a fiber gyro. In principle, all of the pump power reflected from the ring may be reused in the gyro.

If the same power levels and fiber lengths that are used in the squeezer ring are also used in the gyro, nonlinear effects in the gyro must be considered. We have explored this issue in detail in a separate paper [11]. Here we shall merely point out that the nonlinearity in the fiber gyro will cause additional squeezing but in an opposite direction. The squeezing that occurs in the gyro will undo some of the squeezing initially injected.

The analysis is shown diagrammatically in figure 8, using a Mach-Zehnder configuration. If the gyro is linear (figure 8(a)), it is clear that the squeezed vacuum should be oriented along the horizontal direction. In this way, at the gyro's output signal port, the reduced quadrature is along the signal direction.

For a nonlinear gyro, the effect of the $\chi^{(3)}$ nonlinearity will be to pull the elliptical locus of fluctuations toward a circular shape, thereby destroying the squeezing. As shown in the inset of figure 8(b), one must prepare the squeezed vacuum to counterbalance some of the effect of the gyro nonlinearity. The gyro's signal to noise ratio improvement will then be diminished, but not destroyed completely. In fact, much of the noise reduction advantages may be regained by properly designing the relative nonlinearity of the gyro and squeezer rings. For example, if we set the squeezer's nonlinear phase at π the ideal noise reduction will be approximately -15 dB. If the gyro's nonlinearity is then half of the squeezer's, the noise improvement will reduce to -6 dB.

VII CONCLUSIONS

We described the successful observation of squeezed pulsed vacuum, 5±0.3 dB below the shot noise level, generated from a fiber ring interferometer. Noise generated from GAWBS excitations did not appear to damage the squeezing measurements at low frequencies. Further study should determine the exact GAWBS spectra and magnitude for our experimental configuration. If the squeezed vacuum, properly oriented, is injected into a lossless linear interferometer, the interferometer's signal to noise ratio will improve by the noise reduction factor. We considered the utilization of squeezed vacuum in the improvement of the sensitivity of a shot noise limited fiber gyro. In this case the gyro's nonlinearity must be reduced in proportion to the squeezer's nonlinearity.

VIII ACKNOWLEDGEMENTS

The authors thank Lincoln Laboratories for providing the balanced receiver crucial to this experiment. One of the authors [KB] gratefully acknowledges support from Kevin Champagne and Robert Dahlgren of Draper Laboratories, and the generous help of Steve Alexander of Lincoln Laboratories rendered through the course of this experiment. The support of Draper grant DL-H-404179, of NSF EET 8700474, and JSEP contract number DAAL03-89-C-001 are gratefully acknowledged.

REFERENCES

1. R. M. Shelby, M. D. Levenson, S. H. Perlmutter, R. G. De Voe, and D. F. Walls, *Phys. Rev. Lett.*, **57**, 691, (1986).

2. R. M. Shelby, M. D. Levenson, and P. W. Bayer, *Phys. Rev. B*, **31**, 5244, (1985).

3. R. M. Shelby, P. D. Drummond, and S. J. Carter, *Phys. Rev. A*, **42**, 2966, (1990).

4. K. Bergman and H. A. Haus, *Opt. Lett.*, **16**, 663, (1991).

5. M. Shirasaki and H. A. Haus, *J. Opt. Soc. Am. B*, **7**, 30, (1990).

6. C. M. Caves, *Phys. Rev. D*, **23**, 1693, (1981).

7. R. S. Boudurant and H. J. Shapiro, *Phys. Rev. D*, **30**, 2548, (1984).

8. M. Shirasaki and H. A. Haus, *J. Opt. Soc. Am. B*, **8**, 681, (1991).

9. M. Xiao, L. Wu, and H. J. Kimble, *Phys. Rev. Lett.*, **55**, 2520, (1986).

10. P. Grangier, R. E. Slusher, B. Yurke, and A. LaPorta, *Phys. Rev. Lett.*, **59**, 2153, (1987).

11. H. A. Haus, K. Bergman, and Y. Lai, "Fiber Gyro with Squeezed Radiation," accepted for publication in *J. Opt. Soc. Am. B*, (1991).

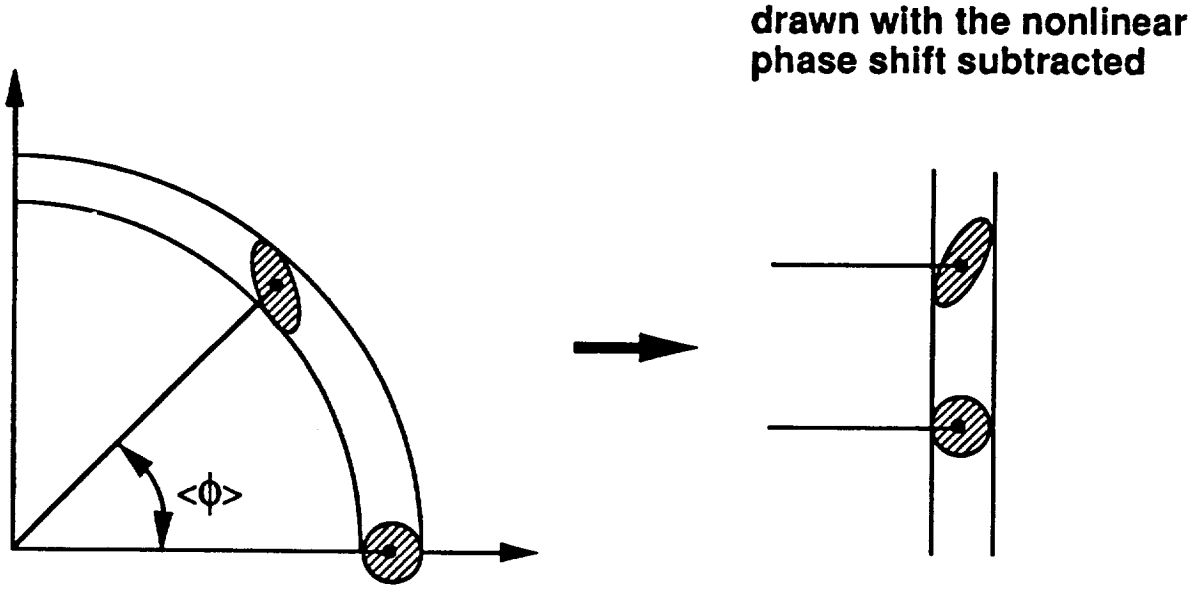

Figure 1 The field's phase insensitive quantum fluctuations are elongated into an ellipse of squeezed noise by the self phase modulation process.

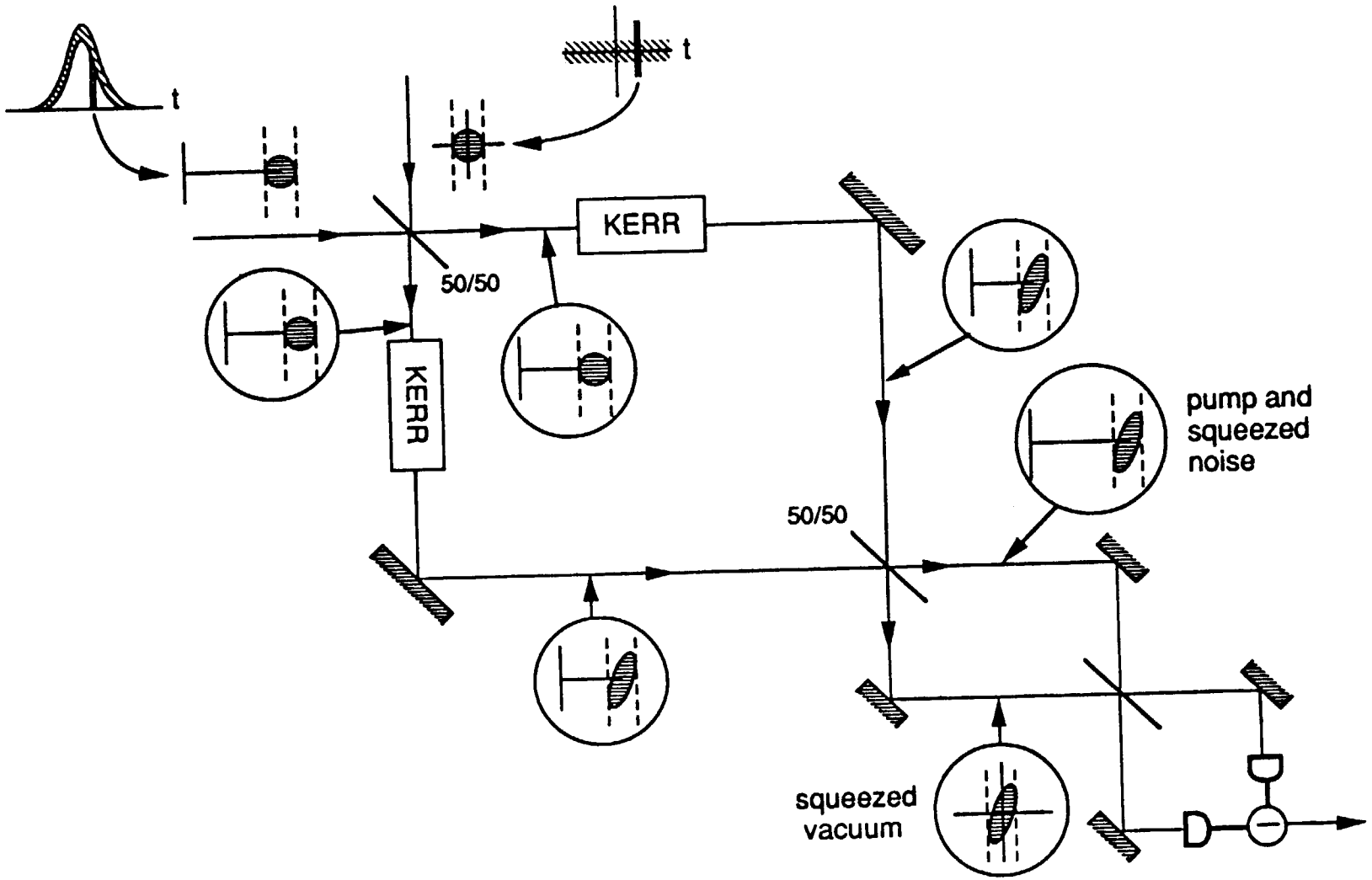

Figure 2 The explanation of squeezing in the Mach-Zehnder interferometric geometry. The pump, separated from the squeezed zero point fluctuations, may be reused as the local oscillator in a homodyne detection.

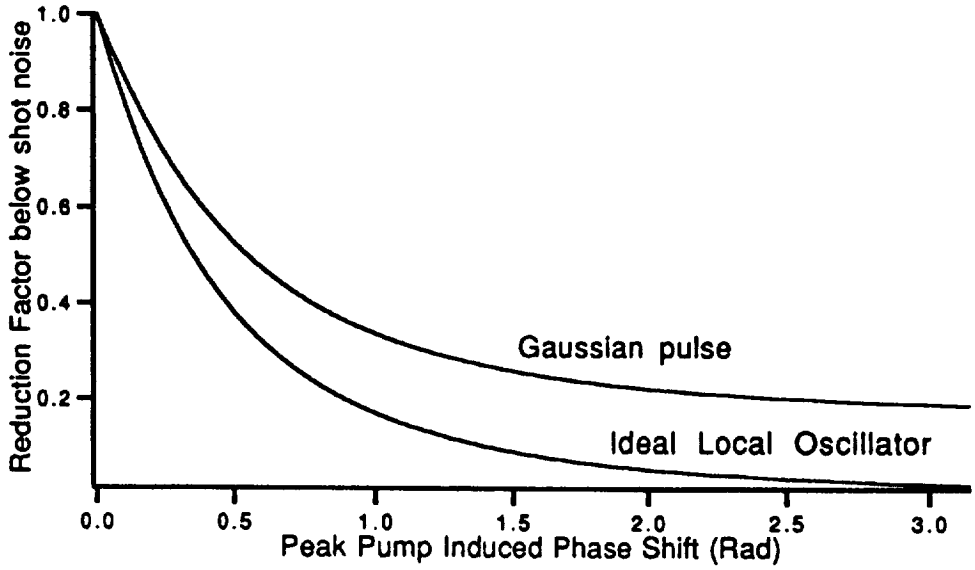

(a)

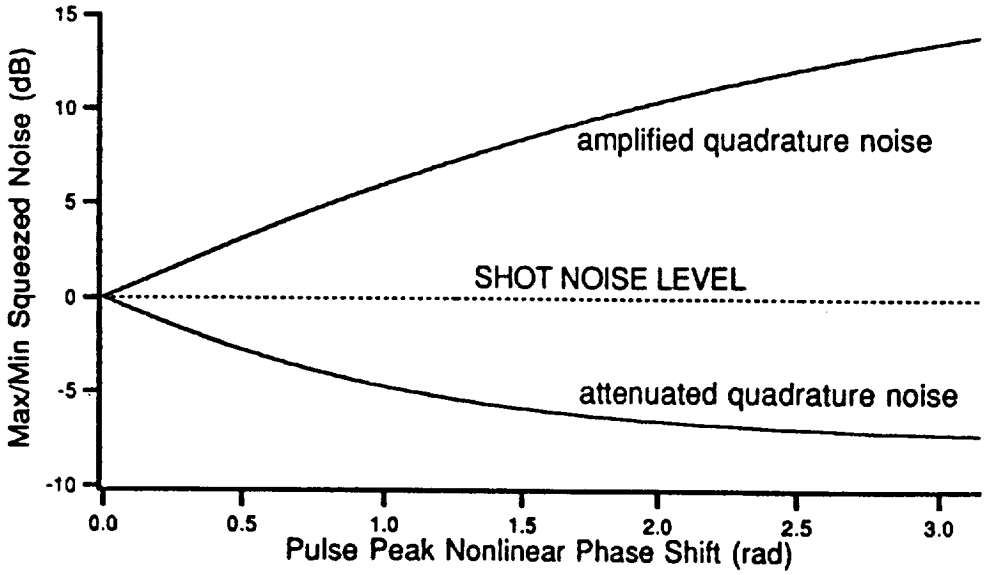

(b)

Figure 3 (a) Expected noise reduction for the ideal and single phase adjusted gaussian pulse cases. (b) Predicted maximum and minimum noise amplitudes for the gaussian local oscillator case, plotted on a dB scale.

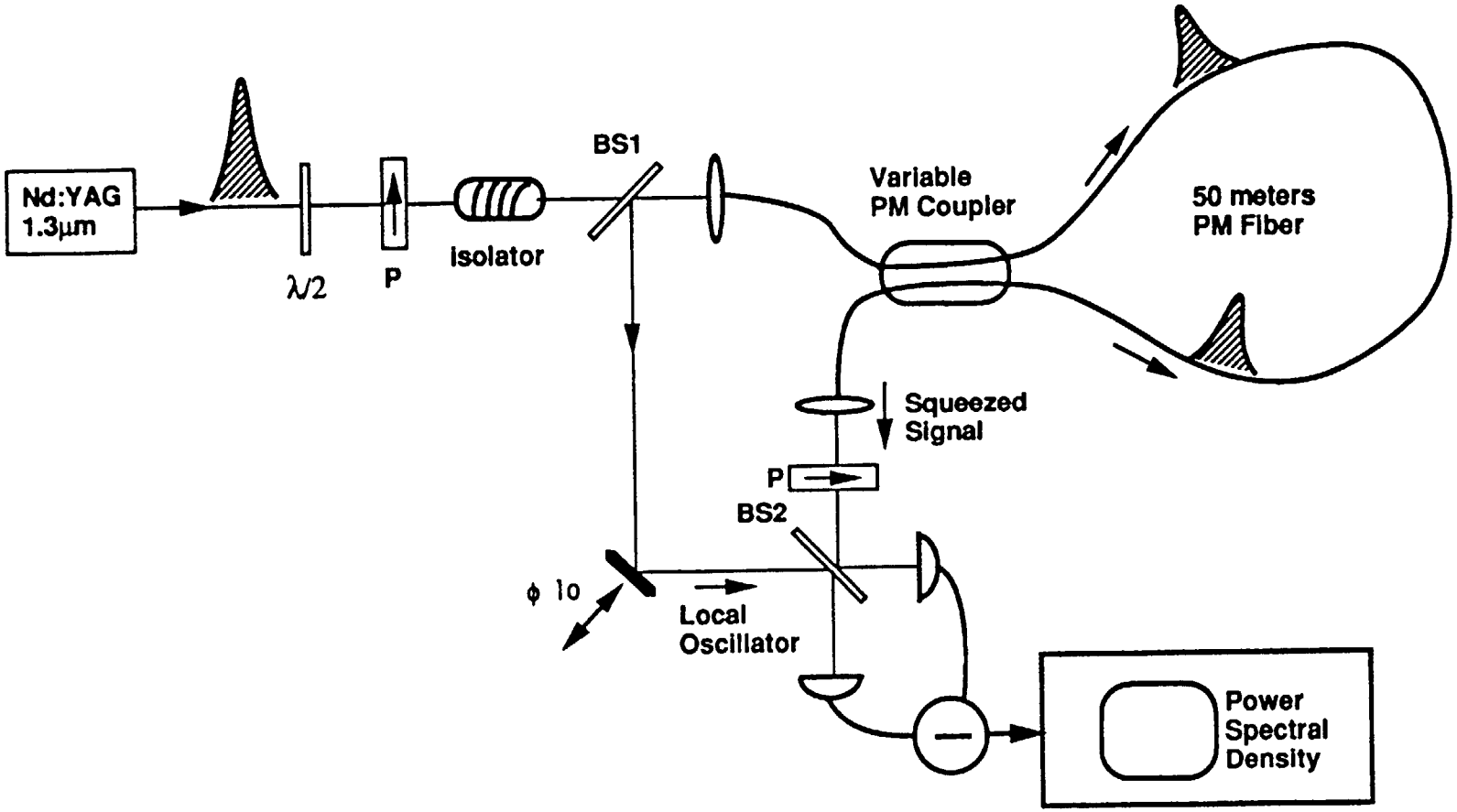

Figure 4 Experimental configuration.

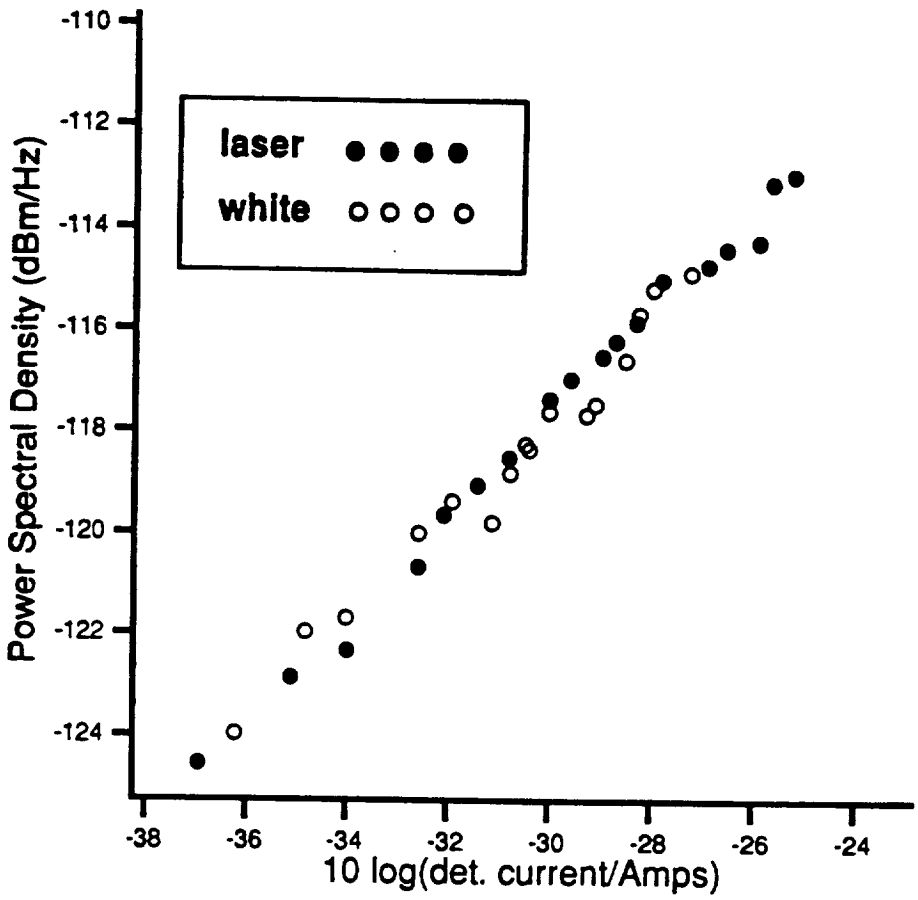

Figure 5 Shot noise calibration using both white light and direct laser excitation.

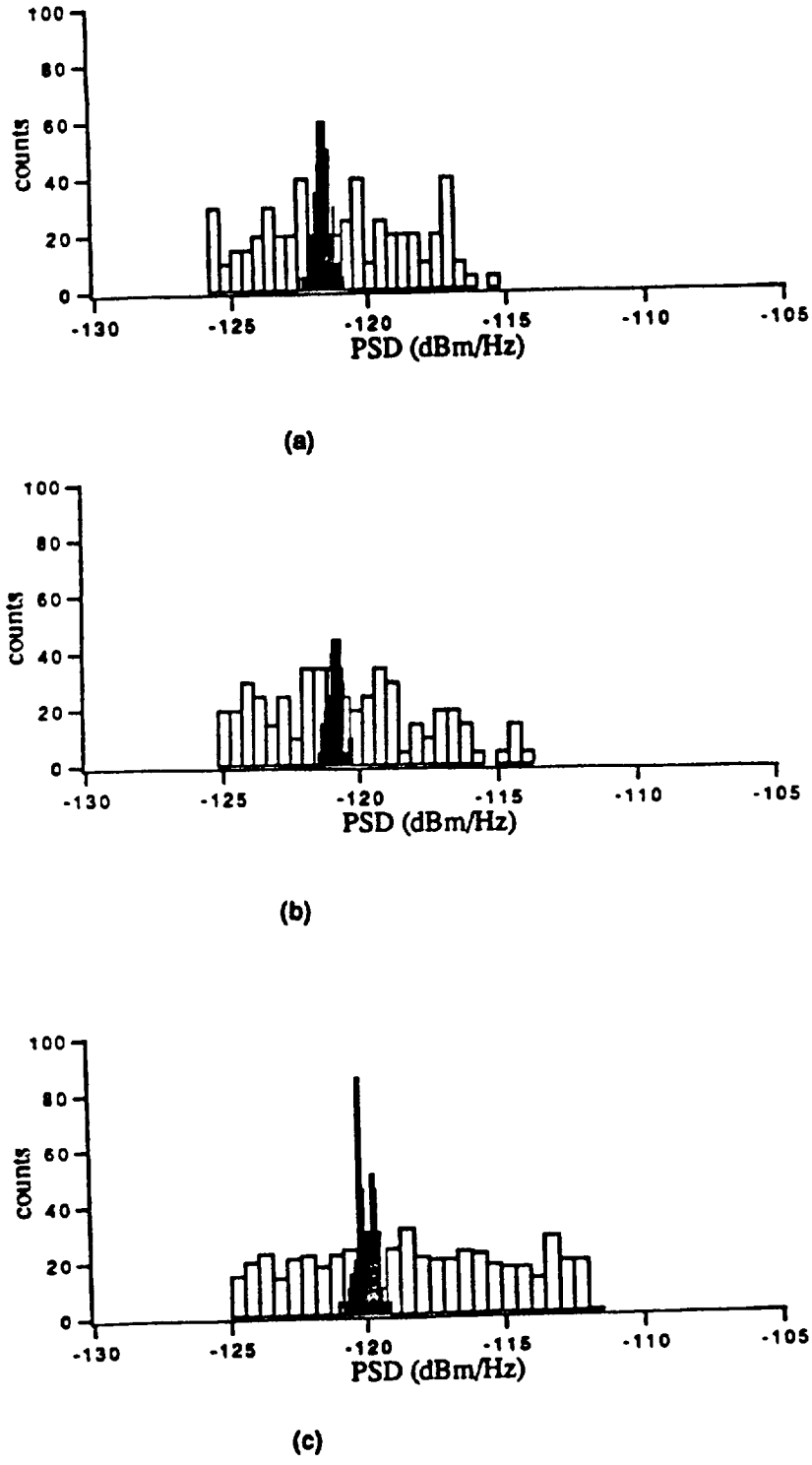

Figure 6 Histograms of PSD readings taken at three separate power levels (a) 60, (b) 85, and (c) 110 mW in each ring direction. The black bars are counts taken with the squeezed signal arm blocked. The white bars are the squeezing PSD measurements.

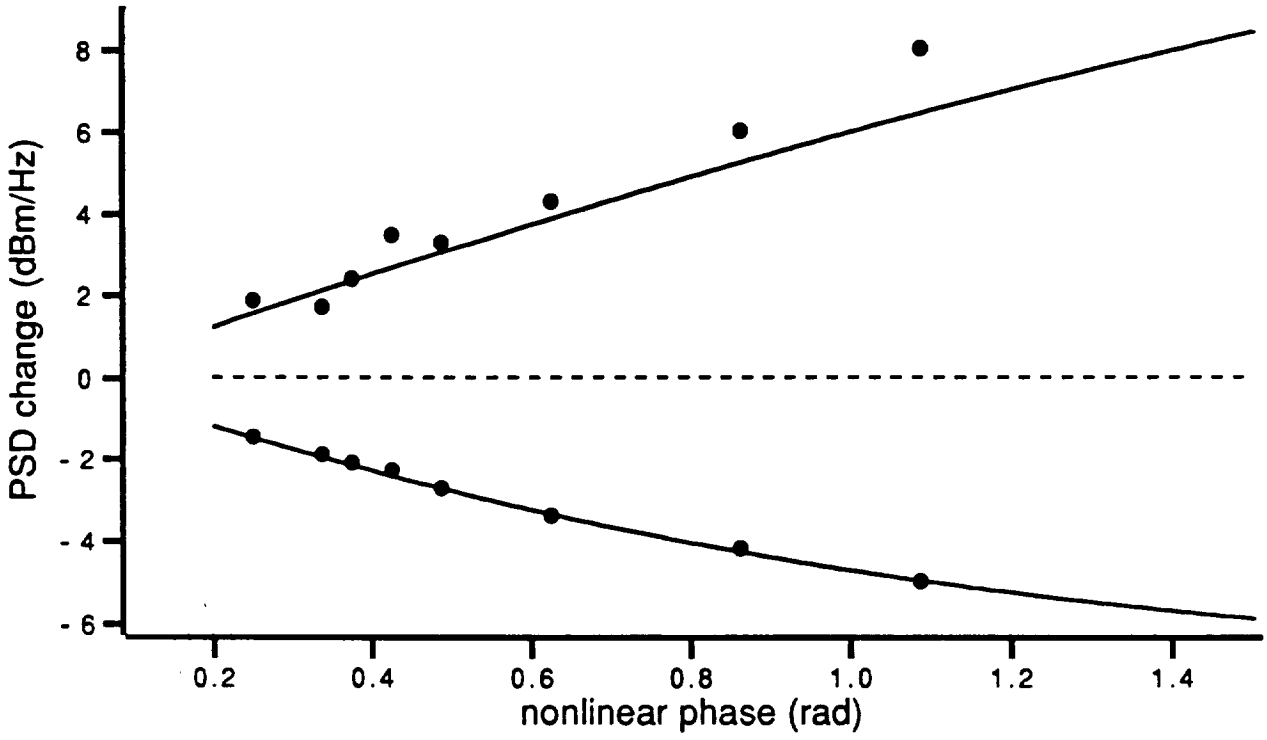

Figure 7 Maximum and minimum values of the PSD readings obtained experimentally (black dots) overlaid on the theoretically predicted curves for the case of a gaussian local oscillator.

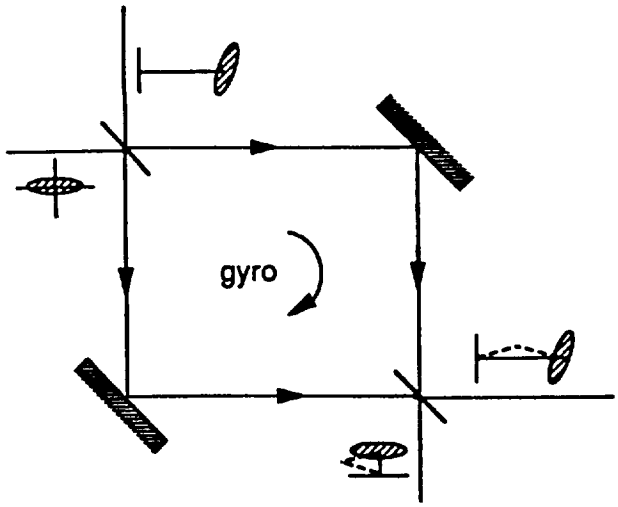

(a)

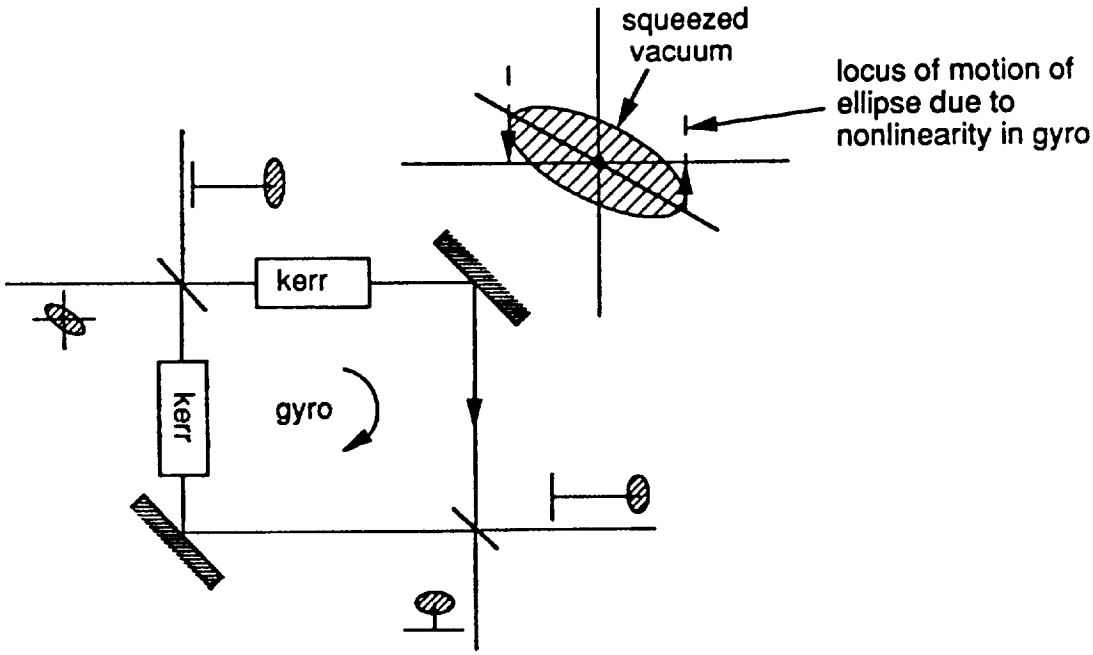

(b)

Figure 8 (a) The linear gyro with squeezed vacuum injected. (b) The nonlinear gyro with phase compensated squeezed vacuum.